Chinese Chemical Letters 36 (2025) 109917

Contents lists available at ScienceDirect

Chinese Chemical Letters

journal homepage: www.elsevier.com/locate/cclet

Orally delivered berberine derivatives for dual therapy in diabetic complications with MRSA infections

Fei-Yan Gao[a,1], Yan Wu[b,1], Ling Yang[a,1], Zhong-Yi Ma[a], Yi Chen[c], Xiao-Man Mao[a], Xu-Fei Bian[a], Pei Tang[c,*], Chong Li[a,*]

[a] Engineering Research Center of Coptis Development & Utilization, Ministry of Education, College of Pharmaceutical Sciences, Southwest University, Chongqing 400715, China
[b] West China Hospital of Stomatology, Sichuan University, Chengdu 610041, China
[c] Sichuan Research Center for Drug Precision Industrial Technology, West China School of Pharmacy, Sichuan University, Chengdu 610041, China

ARTICLE INFO

Article history:
Received 3 February 2024
Revised 15 April 2024
Accepted 22 April 2024
Available online 22 April 2024

Keywords:
8-Alkyl berberine derivatives
Type-2 diabetes mellitus
Methicillin-resistant *Staphylococcus aureus*
Lung infections
Immunoregulation

ABSTRACT

Diabetes mellitus (DM) is a serious health problem in the world, and infections are common complications in diabetic patients, particularly methicillin-resistant *Staphylococcus aureus* (MRSA) infections, which substantially increases mortality in patients. In clinical practice, the treatment of diabetic complication-related infections involves multiple issues such as drug resistance when combining antidiabetic drugs with antibiotics. In this study, a series of derivatives were synthesized with alkyl radicals with different chain lengths substituted at the C8 and C12 positions of berberine, with compounds CY1 and CY3 with good antidiabetic and antibacterial activities screened out after identification. Then, oral liposomes (CY1-Lip and CY3-Lip) were prepared, and their particle sizes, stability, and pharmacokinetics were investigated. In acquired mouse models of diabetes, induced with an acute MRSA lung infection, we demonstrate that CY1-Lip and CY3-Lip can effectively reduce levels of fasting blood glucose (FBG), fasting insulin (FINS), and insulin resistance index among diabetic mice with pneumonia, thus exerting their multi-targets effects. Furthermore, both preparations significantly reduced lung MRSA loads and improved lung tissue lesions, reduced high infiltration of M1 macrophages in lung, and suppressed the expression levels of pro-inflammatory factors such as necrosis factor-α (TNF-α) and interleukin-6 (IL-6). This provides new insights into the clinical treatment of diabetes complicated with pulmonary infections.

Diabetes is a serious health problem in the world, and there were more than 529 million diabetic patients globally by 2021, with an increased prevalence of 6.1% year by year [1–3]. Diabetic patients with long-term metabolic disorders often develop various types of complications involving skin, respiratory tracts, blood, and gastrointestinal tracts [4,5]. Among these complications, lung infection is a common complication and an important cause of death among diabetic patients [6–8]. *In vivo* hyperglycemic conditions of diabetic patients lead to reduced bactericidal capacities of alveolar macrophages and impaired defense functions among hosts, thus resulting in their decreased initial anti-infection abilities. In addition, significantly increased glycation end products can cause vascular endothelial injuries and affect lung ventilation and diffusion functions, thus facilitating colonization, proliferation, and spread of pathogens [9–11]. Some studies have demonstrated that viruses, bacteria, and fungi are important pathogenic microorganisms causing pneumonia. *Staphylococcus aureus* is the most common pathogen colonizing the nasopharynx, with a poor prognosis and a high mortality rate [12].

In current clinical practice, a combined application of hypoglycemic drugs with antibiotics is a primary method for treating diabetes implications with infections [13–15]. However, this therapeutic approach has multiple drawbacks. For instance, a disease type can be treated with only one single drug, leading to repeated medication among patients. Use of antibiotics only after the presence of infection will result in serious consequences due to delayed medication of patients, while long-term use of antibiotics can easily bring about drug resistance [16,17]. Therefore, it is of great significance to develop a drug with dual therapeutic effects of blood glucose reduction and anti-infection, thus improving survival rates and life quality of diabetic patients.

Berberine (BBR), which is an active component isolated from *Coptis rhizome*, possesses multiple hypoglycemic, antibacterial,

* Corresponding authors.
E-mail addresses: peitang@scu.edu.cn (P. Tang), chongli@swu.edu.cn (C. Li).
[1] These authors contributed equally to this work.

https://doi.org/10.1016/j.cclet.2024.109917
1001-8417/

anti-inflammatory, and lipid-lowing pharmacological activities [18,19]. The current study showed that BBR can be used to treat type-2 diabetes mellitus (T2DM) through multiple therapeutic ways, such as repairing injured pancreatic islets, inhibiting gluconeogenesis, and promoting glycolysis [20–23]. And its anti-oxidant and lipid-lowing pharmacological effects can be used as a supplementary method in the treatment of diabetic nephropathy, hepatic steatosis, hyperlipidemia, and other diabetes-related complications. In addition, BBR exhibits varying degrees of inhibitory activity against various microorganisms. However, these antibacterial activities are still considerably lower than those of commonly used clinical antibiotics [24,25]. Therefore, structural modification of BBR is an important approach for the development of BBR derivatives with stronger antibacterial activity and better therapeutic efficacy.

Based on this, we used the BBR structure as a basis and chemically modified it to yield two compounds with stronger antibacterial activity while maintaining the hypoglycemic activity of the BBR screened out. Then, these compounds were used to prepare oral liposomes, which were used in the treatment of diabetic complications with methicillin-resistant *Staphylococcus aureus* (MRSA) lung infection, to explore their anti-MRSA and hypoglycemic mechanisms.

The synthesis routes of target compounds are shown in Fig. 1. Alkyl radicals of varying chain lengths were substituted at the C8 position of BBR through Grignard reaction, with an 8-alkyl berberine derivative (C8-n-BBR) synthesized. Subsequently, bromination was performed at the C12 position of C8-n-BB, with a 12–bromo-8-alkyl berberine derivative (C12-Br-C8-n-BBR) obtained. As shown in Fig. S1 (Supporting information), a total of eight products, namely, CY1 (C8–10-BBR), CY2 (12-Br-C8–10-BBR), CY3 (C8–12-BBR), CY4 (12-Br-C8–12-BBR), CY5 (C8–14-BBR), CY6 (12-Br-C8–14-BBR), CY7 (C8–16-BBR), CY8 (12-Br-C8–16-BBR), and CY9(C8–18-BBR), were synthesized. ^{1}H NMR, ^{13}C NMR, and liquid chromatography-mass spectrometry (LC-MS) (Fig. S2 in Supporting information) were conducted to characterize and confirm all these compounds, with *in vitro* antibacterial activity screening performed to screen out derivatives with strong antibacterial activities. As shown in Table S1 (Supporting information), CY1 and CY3 exhibit excellent antibacterial activities against *C. albicans*, *C. neoformans*, and MRSA (with the same minimum inhibitory concentration (MIC) of 0.25 μg/mL) among all compounds in the test. Then, the inhibitory effects of CY1 and CY3 on *K. pneumoniae*, *P. aeruginosa*, *A. baumannii*, and *S. pneumoniae* were further investigated. The results presented in Table S2 (Supporting information) show that CY1 and CY3 exhibit stronger inhibitory activities against G^{+} pathogens (*S. pneumoniae* and MRSA) than their inhibitory activities against G^{-} pathogens (*K. pneumoniae*, *P. aeruginosa*, and *A. baumannii*). In particular, their inhibitory activities against *S. pneumoniae* are 64 times that of BBR, and their inhibitory activities against MRSA are 512 times higher than those of BBR. The results of the *in vitro* hypoglycemic activity test in Fig. S3 (Supporting information) show that glucose consumption amounts of HepG2 cells significantly decrease with the increases in CY1 and CY3 concentrations, especially under a concentration of 4 μg/mL, those amounts are significantly lower than that of HepG2 cells under the effect of BBR ($P < 0.01$). Therefore, CY1 and CY3 were selected as experimental subjects in further *in vivo* experiments.

In order to improve the solubility of BBR derivatives and protect them from gastrointestinal acid destruction and enzyme degradation, oral liposomes with CY1 and CY3 (CY1-Lip and CY3-Lip) were prepared in this study. The diameters and zeta potentials of CY1-Lip and CY3-Lip were determined by the dynamic light scattering. As shown in Figs. 2A and B, CY1-Lip and CY3-Lip have average diameters of 81.6 ± 3.4 nm and 85.3 ± 5.7 nm, respectively, presenting relatively small particle sizes that are evenly distributed (polymer dispersity index (PDI) = 0.241), which is conducive to the penetration of these two liposomes through the gastrointestinal barrier. Transmission electron microscope (TEM) images showed that CY1-Lip and CY3-Lip present regular spherical morphology, and average zeta potentials was 46.1 ± 2.3 mV and 42.3 ± 3.7 mV, respectively, presenting good dispersion stability. In addition, CY1-Lip and CY3-Lip were effectively encapsulated, with encapsulation efficiency (EE) as high as 87.2% and 89.6%, respectively. As shown in Fig. 2C, particle sizes and encapsulation rates of liposomes remained stable after 72 h in 37 °C temperatures environment during the storage time without obvious drug precipitation. The *in vitro* drug release studies of CY1-Lip and CY3-Lip were carried out in the simulated gastric fluids (SGF) and intestinal fluids (SIF). As shown in Fig. 2D, the cumulative release rate of BBR in SGF reached a value of 90.3% within 2 h. And the cumulative release rates of CY1 and CY3 in SGF reached values higher than 80%, with values of their release rates after a period of 6 h in SIF higher than 90%. Different from this, CY1-Lip and CY3-Lip presented stable release rates of 18.6% and 20.6% after 2 h in SGF, respectively. Transferred to SIF, their release rates reached their maximum values after 24 h and then stabilized, showing no significant variations. This indicates that CY1-Lip and CY3-Lip present some certain sustained release effects in gastric fluid, facilitating the absorption of most drugs into intestines and subsequent systemic circulation. A pharmacokinetic study was performed to investigate the *in vivo* behavior of CY1-Lip and CY3-Lip. The results in Fig. S4 (Supporting information) and Table S3 (Supporting information) show that the half-life and C_{max} of CY1-Lip are 1.31 and 1.33 times those of CY1, respectively, while the half-life and C_{max} of CY3-Lip are 1.4 and 1.25 times those of CY3, respectively. Areas under concentration-time curves ($AUC_{0\text{-}t}$) of these two liposomes are significantly greater than those of their corresponding free drugs. Besides, it also had a better safety profile (Fig. S5 in Supporting information). The results confirm that CY1-Lip

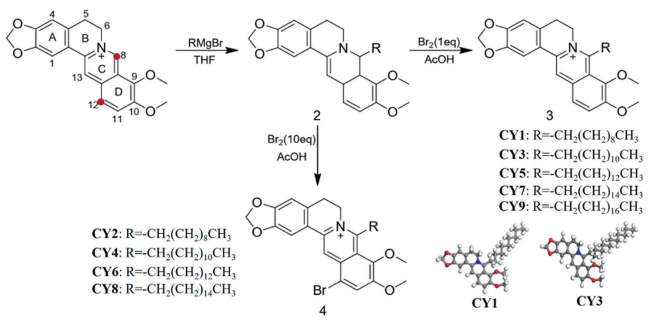

Fig. 1. Synthetic routes of target compounds CY1–CY9.

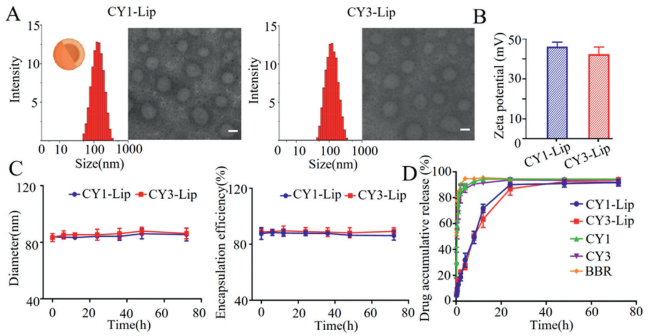

Fig. 2. Characterization of CY1-Lip and CY3-Lip. (A) Size distribution and the representative TEM images of CY1-Lip and CY3-Lip. Scale bar: 50 nm. (B) The average zeta potential of CY1-Lip and CY3-Lip. (C) Stability of CY1-Lip and CY3-Lip (diameter and encapsulation efficiency). (D) *In vitro* release profiles of CY1-Lip and CY3-Lip after 72 h in SGF and SIF. The data were expressed as mean ± SD ($n = 3$).

and CY3-Lip present higher blood drug concentrations than those of BBR and free drugs CY1 and CY3, with significantly improved oral bioavailability.

A T2DM mouse model was established to investigate the *in vivo* therapeutic efficacy of CY1-Lip and CY3-Lip (Fig. S6 in Supporting information). Animal experiments were conducted with approval from the Animal Ethics Committee of southwest university (approval number: IACUC-20210625–02). BBR and metformin hydrochloride (Met) were used as control groups. During the period of drug administration, body weights and blood glucose levels of mice in the CY1-Lip and CY3-Lip groups dropped continuously (Fig. S7 in Supporting information). On the contrary, mice in the T2DM group exhibited continued weight losses, sluggish movements, and yellowish and dull dorsal fur. After the completion of the experiment, mice in the BBR group presented blood glucose levels 1.5 times those of mice in the CY3-Lip group, with their blood glucose levels not significantly different from those of mice in the Met-group. In addition, the CY1-Lip and CY3-Lip groups showed reduced levels of FINS and homeostatic model for assessment of insulin resistance (HOMA-IR) in Fig. 3A, and significantly improved insulin resistance in mice compared to the BBR group. The results of the oral glucose tolerance test (OGTT) test in Fig. 3B and Fig. S8 (Supporting information) show that after oral administration of 2 g/kg glucose, blood glucose levels of mice in all groups rapidly increased within 0.5 h and decreased after another 0.5 h, reflecting the glucose absorption and metabolism processes of organs. The blood glucose of mice in the T2DM group dropped slowly after reaching its peak values, but still kept at a high level within 2 h, indicating seriously impaired glucose tolerance of mice. Mice in all treatment groups present faster blood glucose recovery rates than mice in the T2DM group. Among them, CY1-Lip and CY3-Lip groups presented better therapeutic effects than the BBR group, showing no significantly different effects from those effects of mice in the Met-group, effectively improving impaired glucose tolerance in diabetic mice. The ability of CY1-Lip and CY3-Lip to improve damaged liver, kidney, and pancreatic tissues was further investigated (Fig. 3C). Slight cell-nucleus pyknosis and necrosis occurred among hepatocytes of mice in the T2DM group, with obvious cytoplasmic lipid droplets observed. In the Met-group and BBR group, there are still small amounts of cytoplasmic lipid droplets present in the hepatocytes of mice. Conversely, the treated groups of CY1-Lip and CY3-Lip showed presented similar hepatocyte morphology to that of mice in the control group, with relatively regular cell arrangement and no obvious cell-nucleus pyknosis and cytoplasmic lipid droplets. Meanwhile, it has been observed that renal tubules and glomeruli of mice in the T2DM group presented incomplete morphology and blurred contours, with thickened mesangial matrix and basement membranes. In contrast, mice in the Met, CY1-Lip, and CY3-Lip groups presented clear contours of renal tubules and glomeruli with normal structures. In addition, severe pancreatic lesions were observed among mice in the model group. From images, it can be seen that areas of pancreatic islets significantly decrease, and islet cells are irregularly arranged. Also, partial cell necrosis and wrinkled islet morphology can be observed, with increased boundary division between islet cells and pancreatic acinar cells. Compared with mice in the model group, mice in the Met-and BBR groups presented improved islet structures, but decreased islet areas or increased boundary division between islet cells and pancreatic acinar cells could still be observed. The CY1-Lip and CY3-Lip groups, on the other hand, effectively improved the morphology of pancreatic lesions and pancreatic islets, with uniform cell sizes and regular cell arrangements. At the same time, decreased islet areas were effectively improved among these mice, with similar islet areas to those of normal mice.

A preliminary study on the *in vitro* hypoglycemic mechanism shows that after 1 h of co-incubation with α-glucosidase, starch solution of the control group produced more glucose after hydrolysis, followed by CY1 and BBR group (Fig. 4A). As shown in Fig. S9A (Supporting information), acarbose (Acar) has the strongest inhibitory effect on α-glucosidase under the same concentration. CY1 and CY3 also show relatively good inhibitory effects on α-glucosidase, with the inhibitory rate of CY3 being 1.5 times that of BBR. *In vivo* experimental results show that fasting mice in the control group present greater increased levels of blood glucose than other treatment groups after oral administration of glucose (15 mg/kg), and CY1-Lip, CY3-Lip, and BBR present similar hypoglycemic effects to that of acarbose (Fig. 4B and Fig. S9B in Supporting information). This indicates that the structurally modified BBR derivatives CY1 and CY3 present similar *in vivo* and *in vitro* inhibitory effects on α-glucosidase activity, thereby controlling blood glucose levels of diabetic mice. In addition, as shown in Fig. 4C and Fig. S10A (Supporting information), Met, BBR, CY1-Lip, and CY3-Lip increased AMP-dependent protein kinase (AMPK) and phosphorylation levels in the livers of diabetic mice. CY1-Lip and CY3-Lip showed a significant increase in AMPK activity, which was 1.9 and 1.8 times higher than in the BBR group, respectively. This suggests that CY1-Lip and CY3-Lip can inhibit hepatic fat deposition and improve hepatic insulin sensitivity and insulin resistance by enhancing hepatic AMPK activity. Moreover, the study of drug

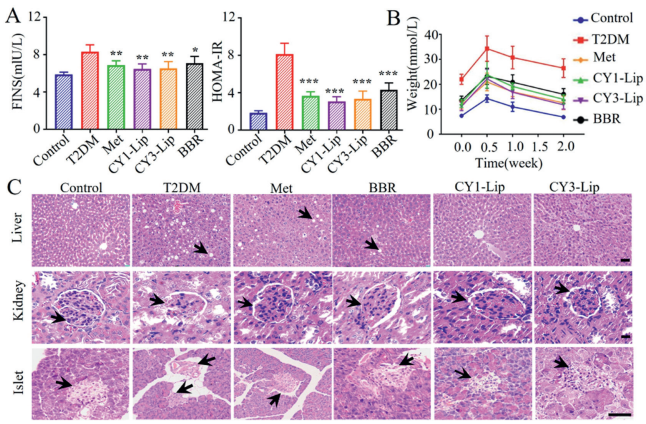

Fig. 3. Evaluation of hypoglycemic efficacy of CY1-Lip and CY3-Lip. (A) FINS and HOMA-IR in normal and diabetic mice after oral administration of CY1-Lip, CY3-Lip and BBR. Saline was used for the control and T2DM group. (B) OGTT blood glucose curve in different group. The data were expressed as mean ± SD ($n = 6$). $^{*}P < 0.05$, $^{**}P < 0.01$, $^{***}P < 0.001$, compared with T2DM group. (C) H&E staining of liver, kidney and pancreatic tissue in each group of mice after treatment. Scale bar: 50 μm.

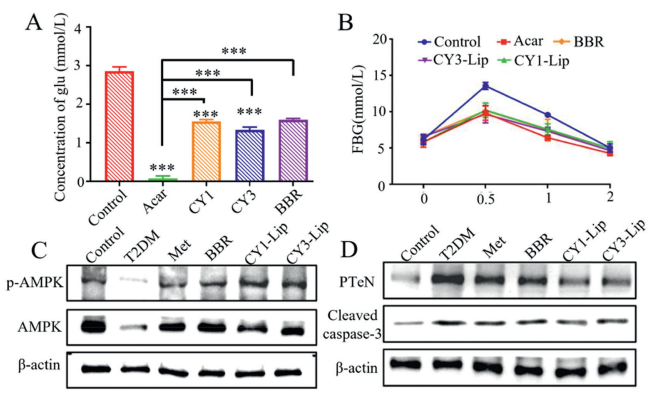

Fig. 4. Glucose-lowering mechanisms of CY1-Lip and CY3-Lip in type 2 diabetes. (A) *In vitro* and (B) *in vivo* α-glucosidase inhibitory effects of CY1, CY3, BBR, and acarbose group. (C) The expression levels of AMPK and p-AMPK proteins in liver tissue for the Western blot (WB) protein band images. (D) The expression levels of PTeN and cleaved caspase-3 proteins in pancreatic tissue for the WB protein band images. The data were expressed as mean ± SD ($n = 3$). $^{***}P < 0.001$.

repairing capacities on impaired pancreatic islets shows that CY1-Lip and CY3-Lip present the strongest negative regulation capacities on phosphatase and tensin homolog (PTeN) and activated caspase-3 level, thus reducing islet damage and restoring islet functions (Fig. 4D and Fig. S10B in Supporting information).

On this basis, *in vivo* antibacterial effectiveness was further studied using the infection models of MRSA, *C. neoformans*, *C. albicans*. All results were obtained in Fig. 5A shows the test results for infected and uninfected samples. Quantitative analysis in Fig. 5B showed that mice treated with CY1-Lip and CY3-Lip showed a reduction in lung MRSA levels of 1.3 and 1.2 orders of magnitude, respectively, compared to untreated mice. In contrast, mice in the BBR group exhibit the weakest inhibitory effects on their lung MRSA levels, with no differences from those effects presented by mice not treated. This indicates that CY1-Lip and CY3-Lip have strong *in vivo* antibacterial effects, which can be used to cure lung infections induced by MRSA effectively. Lung *C. neoformans* bacterial load and kidney *C. albicans* load quantification were performed in Figs. 5C and D, respectively. Compared to untreated mice, the *C. neoformans* load in the lungs of mice infected with CY1-Lip and CY3-Lip decreased by 1.4 and 1.9 orders of magnitude, respectively, while the BBR group showed a reduction of 0.4 orders of magnitude in the lungs. In terms of *C. albicans*, BBR presented the poorest therapeutic effect, with loads in the kidneys of mice in the BBR group reduced by only 0.2 orders of magnitude. Meanwhile, the levels of *C. albicans* in the kidneys of mice in the CY1-Lip and CY3-Lip groups were reduced by 1 and 1.3 orders of magnitude, respectively, and the efficacy was significantly better than that of BBR. These results indicated that fungal treatment of *in vivo* infection afforded good therapeutic outcome by CY1-Lip and CY3-Lip. Minimum eradication concentrations of CY1, CY3, vancomycin, and BBR on MRSA biofilms individually were examined in Table S4 (Supporting information). The minimum biofilm eradication concentration (MBEC) values were 4 μg/mL for CY1 and CY3, revealed a higher biofilm inhibitory activity on the formation of MRSA biofilms. Furthermore, the inhibitory capacities of all drugs on MRSA biofilms were evaluated in this study. As shown in Fig. 5E, under an MIC concentration, inhibitory rates of CY1 and CY3 on biofilms reached a value above 50%. Meanwhile, under a concentration of over 2MIC, biofilms were almost completely eliminated, presenting significantly different inhibitory performances on MRSA biofilms among mice in the drug and control groups. On the contrary, under a concentration of 4MIC, the inhibitory rate of BBR on biofilms reached a level of only around 50%, indicating significantly stronger inhibitory capacities of CY1 and CY3 on MRSA biofilms than that of BBR.

A T2DM complication model with MRSA lung infection was established to further reveal the *in vivo* therapeutic effects and mechanisms (Fig. 6A). MRSA-infected mice in all groups presented a decreasing trend in body weight, with mice in the T2DM&MRSA group, consecutively followed by mice in the Met, BBR, CY1-Lip, and CY3-Lip groups, presented the fastest losses of body weights. In addition, blood glucose levels in the mice decreased continuously after administration, with the CY1-Lip and CY3-Lip groups showing significantly lower fasting glucose levels than the T2DM&MRSA group (Fig. S11 in Supporting information). Serum insulin levels and insulin resistance indexes of mice with T2DM&MRSA group were significantly higher than those of mice in the control group, indicating severe insulin resistance among these mice. After a period of 30-day continuous drug administration, compared with mice in the BBR and Met-groups, mice in the CY1-Lip and CY3-Lip groups presented significantly reduced serum insulin levels and insulin resistance indexes in Fig. 6B, effectively improving insulin resistance in the model group mice and increasing the sensitivity of the body tissues to insulin. The lung colony loads in Figs. 6C and D shown that mice in the T2DM&MRSA group presented the highest loads of lung bacteria, with an MRSA load value of (4.42 ± 0.20) Log_{10} colony-forming units (CFU)/g tissue. Mice in all drug administration groups showed some certain reduced levels of lung colony loads, with an MRSA load value of (3.96 ± 0.15) Log_{10} CFU/g tissue among mice in the Met-group, representing an approximate decrease of 0.5 orders of magnitude compared with the load value among mice in the untreated group. The reason lies in that *in vivo* high glucose environments can promote the growth of MRSA, while Met-can inhibit the rapid proliferation of MRSA by lowering levels of blood glucose. Mice in the BBR group exhibited an MRSA load value of (3.49 ± 0.14) Log_{10} CFU/g tissue, with better efficacy than the Met-group, indicating that BBR has certain antibacterial effects in addition to the good hypoglycemic effect. CY1-Lip and CY3-Lip showed significantly better efficacy than Met- and BBR, with CY3-Lip reducing lung colony numbers in mice by about three orders of magnitude. These results indicate that with a strong *in vivo* antibacterial effect, CY3-Lip can be used to cure lung infections of diabetic mice induced by MRSA effectively.

In addition, hematoxylin-eosin staining (H&E) staining of lung tissue slices further confirmed the above observations (Fig. 6E). The

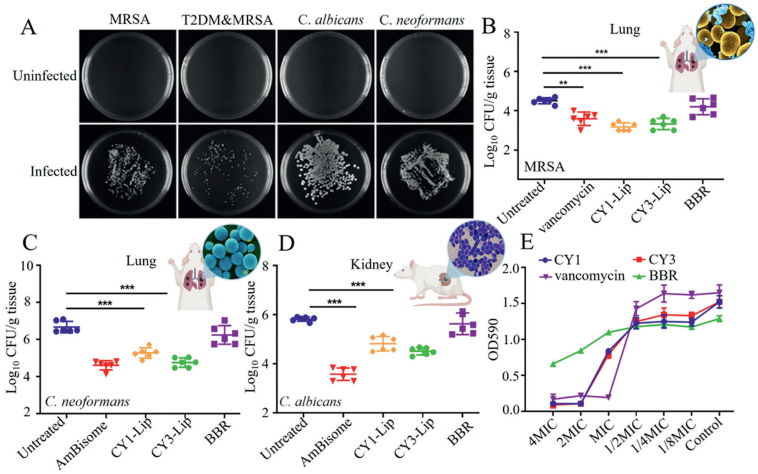

Fig. 5. Evaluation of treatment of Gram-positive bacterial infections in mice. (A) The illustration and bacterial colony counts for MRSA, diabetic MRSA, *C. neoformans* and *C. albicans* infections. (B) Pulmonary bacterial colony counts after administration in mice infected with MRSA. (C) Pulmonary bacterial colony counts after administration in mice infected with *C. neoformans*. (D) Renal bacterial colony counts after administration in mice infected with *C. albicans*. The data were expressed as mean ± SD ($n = 6$). $^{**}P < 0.01$, $^{***}P < 0.001$. (E) Antibiofilm effect of CY1, CY3, BBR and vancomycin on MRSA.

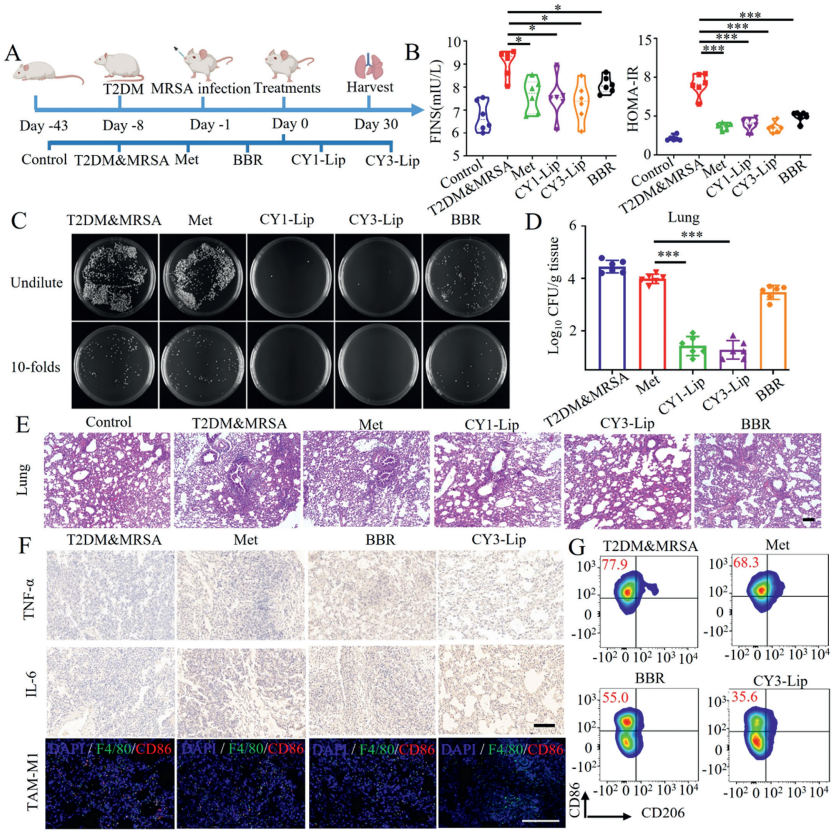

Fig. 6. Evaluation of CY1-Lip and CY3-Lip in the treatment of a diabetic mouse MRSA infection. (A) Schematic diagram of diabetic mouse with MRSA infection. (B) The level of FINS and HOMA-IR in different groups after oral administration. (C) The images and (D) bacterial colony count of different treatment groups in diabetic mouse MRSA infection. The data were expressed as mean ± SD ($n = 6$). $^{*}P < 0.05$, $^{***}P < 0.001$. (E) H&E staining of lung tissue in each group. Scale bar: 100 μm. (F) Images of immunohistochemistry (TNF-α and IL-6) and TAM (F4/80-green and CD86-red) staining of lung tissues of the mice treated with different drugs. Scale bar: 100 μm. (G) Representative flow cytometry dot plots of TAMs ($CD86^{+}CD206^{+}$) in lungs ($n = 3$).

lung cells from the disease model group of mice experienced extensive necrosis, which were irregularly distributed. And congestion was observed in some of the pulmonary alveoli and bronchi, and significant infiltration of a large number of inflammatory cells throughout the lung tissue. Lung sections of mice in the Met-group presented almost the same results as those of mice in the model group, indicating that Met-has hardly any therapeutic effect on lung infections of diabetic mice. Compared with mice in the Met- and BBR groups, mice treated with CY1-Lip and CY3-Lip interventions presented significantly improved pathological conditions of lungs, with reduced expansion of their pulmonary alveoli and lung cells uniformly arranged, as well as significantly improved infiltration of inflammatory cells. Taken together, CY1-Lip and CY3-Lip can be used to cure MRSA-induced diabetic complications with lung infections. In particular, CY3-Lip can be used to improve lung tissue lesions and cell necrosis of diabetic mice with lung infections significantly.

We further analyzed the alterations of the lung microenvironment in CY3-Lip-treated mice as well as the mechanisms by which CY3-Lip induces pulmonary immunoregulation. Macrophages are key immune cells playing a crucial immunosuppressive role in the inflammatory microenvironment [26,27]. As shown in Fig. 6F, *in vivo* microenvironments of diabetic mice are conducive to high infiltration of M1 macrophages in their lungs, while mice in the CY3-Lip group present significantly reduced expression levels of M1 macrophages. Compared with mice in the T2DM&MRSA group, mice treated with CY3-Lip presented significantly reduced secretion levels of pro-inflammatory cytokines necrosis factor-α (TNF-α) and interleukin-6 (IL-6), thus reducing sustained and serious infections. Flow cytometry was used to verify changes in M1-subtyp e macrophages in the lung tissues of mice after CY3-Lip intervention in Fig. 6G. The results show that mice in the T2DM&MRSA group presented a much higher proportion of M1 macrophages (Q1: 77.9%) than that of mice in the BBR group (Q1: 55.0%), while the M1 macrophage proportion of lung tissues of mice treated with CY3-Lip decreased to a value of 35.6. These results show that CY3-Lip has an immunomodulatory capacity to reduce the polarization of macrophages towards the M1 phenotype.

In summary, we synthesized a series of derivatives of BBR in this study. Among them, compounds CY1 and CY3 that were screened out can retain the excellent hypoglycemic activity of BBR and present stronger inhibitory activities against MRSA, with an MIC value of 0.25 μg/mL. On the basis of these two compounds, oral liposomes CY1-Lip and CY3-Lip were prepared, and *in vivo* therapeutic efficacy and mechanisms on type-2 diabetes and type-2 diabetic complications with MRSA lung infections were further investigated. The study results show that compared with BBR, CY1-Lip and CY3-Lip can better give full play to their multi-target effects, significantly improving impaired glucose tolerance of diabetic mice. Moreover, these two liposomes can significantly reduce MRSA loads in the lungs of mice and present stable antibacterial and immunomodulating functions, thus providing a new strategy for clinical treatments of diabetic complications with infections.

Declaration of competing interest

The authors declare that they have no known competing financial interests or personal relationships that could have appeared to influence the work reported in this paper.

CRediT authorship contribution statement

Fei-Yan Gao: Writing – review & editing, Writing – original draft, Visualization, Validation, Methodology, Funding acquisition, Data curation. **Yan Wu:** Writing – review & editing, Writing – original draft, Visualization, Validation, Methodology, Data curation. **Ling Yang:** Writing – original draft, Investigation, Validation, Data curation. **Zhong-Yi Ma:** Validation, Data curation. **Yi Chen:** Validation, Data curation. **Xiao-Man Mao:** Formal analysis, Data curation. **Xu-Fei Bian:** Formal analysis, Data curation. **Pei Tang:** Conceptualization, Methodology, Writing – review & editing. **Chong Li:** Conceptualization, Methodology, Funding acquisition, Writing – original draft, Writing – review & editing.

Acknowledgments

We acknowledge financial support provided by Young Scientists Fund of the National Natural Science Foundation of China (No. 32201086), Postdoctoral Science Foundation of Chongqing Natural Science Foundation (No. cstc2021jcyj-bshX0125), and the project for Chongqing University Innovation Research Group, Chongqing Education Committee (No. CXQT20006).

Supplementary materials

Supplementary material associated with this article can be found, in the online version, at doi:10.1016/j.cclet.2024.109917.

References

[1] S. Chatterjee, K. Khunti, M.J. Davies, Lancet 389 (2017) 2239–2251.
[2] D.J. Magliano, J.W. Sacre, J.L. Harding, et al., Nat. Rev. Endocrinol. 16 (2020) 321–331.
[3] K.L. Ong, L.K. Stafford, S.A. McLaughlin, et al., Lancet 402 (2023) 203–234.
[4] H. Zhao, Y. Zheng, L. Zhu, et al., Chin. Chem. Lett. 33 (2022) 3139–3143.
[5] X. Wang, C. Ding, Z. Zhang, et al., Chin. Chem. Lett. 34 (2023) 107951.
[6] W.J. Guan, Z.Y. Ni, Y. Hu, et al., N. Engl. J. Med. 382 (2020) 1708–1720.
[7] E. Ortega, R. Corcoy, M. Gratacòs, et al., BMJ Open 11 (2021) e051237.
[8] E.L. Feldman, B.C. Callaghan, R. Pop-Busui, et al., Nat. Rev. Dis. Primers. 5 (2019) 42.
[9] K. Hodgson, J. Morris, T. Bridson, B. Govan, C. Rush, N. Ketheesan, Immunology 144 (2015) 171–185.
[10] V. Bezzerri, F. Piacenza, N. Caporelli, et al., Respir. Res. 20 (2019) 32.
[11] A. Vargas, G. Garcia, K. Rivara, et al., Int. J. Mol. Sci. 24 (2023) 2143.
[12] H.J. Stacey, C.S. Clements, S.C. Welburn, J.D. Jones, Acta Diabetol. 56 (2019) 907–921.
[13] S.P. Nobs, A.A. Kolodziejczyk, L. Adler, et al., Nature 624 (2023) 645–652.
[14] M.J. Holzmann, B. Rathsman, B. Eliasson, et al., J. Am. Coll. Cardiol. 65 (2015) 1644–1652.
[15] A. Giaccari, A. Solini, S. Frontoni, S. Del Prato, Diabetes Care 44 (2021) 647–654.
[16] S.G. Swinnen, A.C. Simon, F. Holleman, J.B. Hoekstra, J.H. Devries, Cochrane Database Syst. Rev. 7 (2011) Cd006383.
[17] M. Otto, Annu. Rev. Microbiol. 64 (2010) 143–162.
[18] Y. Chen, Z. Zheng, J. Wang, et al., Int. J. Biol. Sci. 14 (2018) 682–692.
[19] W. Kong, J. Wei, P. Abidi, et al., Nat. Med. 10 (2004) 1344–1351.
[20] H.A. Jung, N.Y. Yoon, H.J. Bae, B.S. Min, J.S. Choi, Arch. Pharm. Res. 31 (2008) 1405–1412.
[21] X. Bian, L. He, G. Yang, Bioorg. Med. Chem. Lett. 16 (2006) 1380–1383.
[22] S. Zhang, X. Wang, W. Yin, et al., Bioorg. Med. Chem. Lett. 26 (2016) 4799–4803.
[23] J.T. Wang, J.G. Peng, J.Q. Zhang, et al., Bioorg. Med. Chem. Lett. 29 (2019) 126709.
[24] X.F. Shang, C.J. Yang, S.L. Morris-Natschke, et al., Med. Res. Rev. 40 (2020) 2212–2289.
[25] A. Zagrebaev, V. Butova, A. Guda, et al., New. J. Chem. 48 (2024) 268–280.
[26] D.G. DeNardo, B. Ruffell, Nat. Rev. Immunol. 19 (2019) 369–382.
[27] T.A. Wynn, A. Chawla, J.W. Pollard, Nature 496 (2013) 445–455.